Case Report

Mapping Sanfilippo Syndrome: A Multisystem Clinicopathological Autopsy

Mioara-Florentina Trandafirescu , Elena-Roxana Avădănei * , Nina Filip , Catalina Iulia Săveanu , Iolanda Foia , Vasilica Toma , Livia Genoveva Baroi , Dana-Teodora Anton-Paduraru , Ștefana Maria Moisă , Ludmila Lozneanu

Posted Date: 26 March 2026

doi: 10.20944/preprints202603.2091.v1

Keywords: mucopolysaccharidosis type III; Sanfilippo syndrome; lysosomal storage disorder; autopsy; histopathology; glycosaminoglycans; foam cells; multisystem involvement

 doi:10.20944/preprints202603.2091.v1

Case Report

Mapping Sanfilippo Syndrome: A Multisystem Clinicopathological Autopsy

Mioara-Florentina Trandafirescu, Elena-Roxana Avădănei *, Nina Filip, Catalina Iulia Saveanu, Iolanda Foia, Vasilica Toma, Livia Genoveva Baroi, Dana-Teodora Anton-Paduraru, Stefana Maria Moisa, Ludmila Lozneanu

"Grigore T. Popa" University of Medicine and Pharmacy, 16 University Street, 700115 Iasi, Romania

* Correspondence: elena.avadanei@umfiasi.ro

Abstract

Background/Objectives: Mucopolysaccharidosis type III (MPS III, Sanfilippo syndrome) is an autosomal recessive lysosomal storage disorder caused by deficiencies in enzymes required for heparan sulfate degradation. While primarily recognized for its devastating neurodegenerative course, the systemic extent of glycosaminoglycan (GAG) accumulation remains under-characterized. This study aims to provide a detailed multisystemic pathological mapping of MPS III to challenge the traditional "brain-only" disease paradigm and highlight the clinical relevance of extracerebral involvement. **Methods:** We present a comprehensive clinicopathological analysis of a 15-year-old female patient with a history of profound neuropsychomotor delay, refractory epilepsy, and spastic tetraplegia. Following her death due to terminal bronchopneumonia during palliative care, a complete forensic and pathological autopsy was conducted. Tissue samples from all major organ systems were processed using routine Hematoxylin-Eosin (HE) staining alongside specialized histochemical stains to identify intracellular storage products. **Results:** Macroscopic evaluation revealed significant diffuse cerebral atrophy, meningoencephalic edema, cardiac valvulopathy with compensatory myocardial remodeling, and hepatosplenomegaly. Furthermore, erosive gastrointestinal lesions and degenerative renal changes were identified. Histopathological examination confirmed widespread cytoplasmic vacuolization across diverse cell populations, including neurons, hepatocytes, renal tubular cells, and the reticuloendothelial system. These findings demonstrate that GAG deposition is a generalized process affecting nearly every parenchymal structure. **Conclusions:** Although neurological decline dominates the clinical phenotype, our findings underscore that MPS III is a true systemic storage disorder. Significant involvement of the cardiovascular and visceral systems contributes to the disease's complexity and mortality. This case reinforces the critical diagnostic value of a comprehensive autopsy in delineating the full morphological spectrum of Sanfilippo syndrome, providing essential insights for multidisciplinary management.

Keywords: mucopolysaccharidosis type III; Sanfilippo syndrome; lysosomal storage disorder; autopsy; histopathology; glycosaminoglycans; foam cells; multisystem involvement

1. Introduction

Mucopolysaccharidoses constitute a heterogeneous group of inherited metabolic disorders caused by deficiencies of lysosomal enzymes responsible for the degradation of glycosaminoglycans [1,2]. MPS III (mucopolysaccharidosis type III) results from impaired catabolism of heparan sulfate due to mutations affecting one of several specific enzymes, leading to gradual intralysosomal substrate accumulation and cellular dysfunction [3,4]. Each of this enzyme determinates a different tipe of MPS III (IIIA, IIIB, IIIC, IIID and IIIE), as follows: heparan N-sulphatase in MPS IIIA, α-N-acetylglucosaminidase (NAGLU) in MPS IIIB, heparan acetyl CoA: α-glucosaminide N-

 doi:10.20944/preprints202603.2091.v1

acetyltransferase (HGSNAT) in MPS IIIC, N-acetyl glucosamine sulfatase (GNS) in MPS IIID, and N-glucosamine 3-O-sulfatase (arylsulfatase G or ARSG) in MPS IIIE. The fifth proposed subtype, MPS IIIE, appears to exhibit a clinical phenotype distinct from the classic forms of MPS III [5].

Lysosomal impairment disrupts cellular homeostasis, promotes chronic neuroinflammation, and triggers ongoing neuronal loss [2,6,7]. Clinically, patients typically present with developmental delay followed by cognitive regression, behavioral disturbances, epilepsy, and progressive motor deterioration [8–10]. Diagnostic delay and misdiagnosis of idiopathic developmental delay, ADHD, or Autism Spectrum Disorder (ASD) are frequently reported [9,11]. Although the central nervous system is considered the primary target, increasing evidence suggests that systemic somatic involvement may be underrecognized and insufficiently characterized at the morphopathological level [12–14].

Unlike MPS types I and II, where somatic manifestations are clinically dominant [15,16], MPS III is traditionally characterized as a primary neurodegenerative condition with more subtle visceral features [17].

Therapeutic limitations in mucopolysaccharidosis type III result from the inability of conventional enzyme replacement therapies to cross the blood–brain barrier, thereby restricting central nervous system efficacy and maintaining the predominantly neurodegenerative course of the disease. However, imaging and laboratory investigations frequently demonstrate hepatosplenomegaly, cardiac abnormalities, and progressive multisystem changes [12,18–20], indicating broader organ involvement. Although overall survival is largely determined by progressive neurological decline, quality of life and acute clinical complications are frequently influenced by systemic dysfunction, particularly cardiac and respiratory involvement [21,22].

In this context, post-mortem examination remains a crucial tool for accurately assessing disease burden and correlating clinical manifestations with their histopathological substrate [2].

The aim of the present study was to provide a detailed macroscopic and microscopic characterization of organ involvement in an advanced case of MPS III, emphasizing the systemic impact of this disorder.

Case Presentation

A 15-year-old female patient with advanced neurodegenerative encephalopathy secondary to mucopolysaccharidosis type IIIA (MPS IIIA) was admitted to the palliative care unit of the Children's Emergency Hospital “Sf. Maria” in Iași by inter-hospital transfer from a tertiary medical center in another city due to progressive clinical deterioration. The patient had been institutionalized in a residential care facility, where she had been institutionalized for several years because of her complex medical and social needs.

The diagnosis of MPS IIIA had been established in early childhood, at approximately 3 years of age, following developmental regression and behavioral disturbances. Biochemical investigations revealed increased urinary glycosaminoglycan excretion with predominance of heparan N-sulfatase, and enzymatic assays confirmed the specific lysosomal deficiency.

Her clinical course followed the typical advancing neurodegenerative trajectory of Sanfilippo syndrome. Early manifestations included language delay, cognitive stagnation, marked hyperactivity, behavioral dysregulation, and significant sleep disturbances characterized by fragmented sleep and nocturnal agitation. During mid-childhood, she developed progressive loss of previously acquired skills, worsening intellectual disability, and refractory epilepsy or drug-resistant epilepsy. Motor impairment gradually ensued, with increasing spasticity, gait instability, and eventual loss of independent ambulation, progressing toward severe spastic tetraplegia. Bulbar dysfunction with dysphagia and recurrent aspiration episodes led to the imperative usage of enteral nutritional support via percutaneous endoscopic gastrostomy.

By adolescence, the patient reached a terminal stage, characterized by a non-verbal state, bedridden status, and total dependence on attentive care in order to survive. These clinical manifestations reflect the relentless systemic accumulation of GAGs, leading to the extensive multisystem involvement subsequently documented during post-mortem examination.

 doi:10.20944/preprints202603.2091.v1

2. Materials and Methods

A complete autopsy was performed according to standard protocol. The study was conducted in accordance with the Declaration of Helsinki and approved by the Ethics Committee of Children's Emergency Hospital "Sf. Maria" in Iași (March 2026). Written informed consent was obtained from the patient's legal guardians for the publication of this case report and any accompanying images.

Major organs were systematically examined macroscopically, and representative tissue samples including the central nervous system, heart, lungs, liver, spleen, kidneys, pancreas, gastrointestinal tract, and aorta were harvested. These samples were fixed in 10% buffered formalin, paraffin-embedded, and sectioned at 4–5µm.

For histopathological analysis, routine Hematoxylin-Eosin (H&E) staining, Masson's trichrome stain, Sharlach stain and periodic acid-Schiff (PAS) stain were used. Three independent pathologists (M.F.T., E.R.A. and L.L.) examined the histological slides and identified the microscopic lesions.

Additionally, lipid accumulation within subendothelial foamy macrophages of the aorta was evaluated using Scharlach staining on selected sections.

3. Results

3.1. Macroscopic Findings

The patient showed marked malnutrition with generalized muscle wasting and severe osteoarticular contractures. External examination revealed synophrys (confluent eyebrows) and coarse hair texture, phenotypic features compatible with the dysmorphic characteristics described in certain lysosomal storage disorders.

The cranial vault thickness measured approximately 10mm, markedly exceeding the expected reference range for a 15-year-old adolescent (approximately 5–6mm), suggesting skull remodeling associated with lysosomal storage disease (Figure 1a).

The brain showed marked encephalomalacia or global cerebral atrophy with widened sulci, meningeal congestion, cerebral edema, and ventricular dilatation, reflecting advanced neurodegeneration. At post-mortem analysis, the brain weighed 910g, substantially below the normal reference range for a 15-year-old adolescent female (approximately 1200–1350g), reflecting terminal-stage neurodegeneration (Figure 1b and 1c).

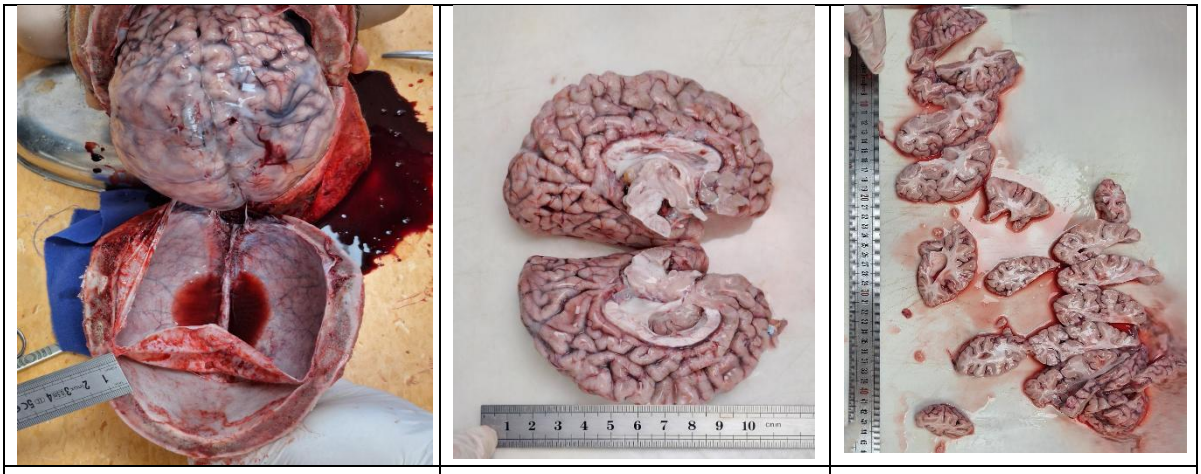

(a)	*(b)*	*(c)*

Figure 1. Gross appearance of the brain: **(a)** thickness of the cranial vault, cerebral edema, and vascular congestion, **(b)** ventricular dilatation and cortical thinning (sagittal slices), **(c)** parenchymal changes associated with advanced neurodegeneration (coronal slices).

 doi:10.20944/preprints202603.2091.v1

The heart displayed cardiomegaly secondary to left ventricular hypertrophy and fibrous thickening of the mitral and aortic valves. The heart weight was 450g, markedly exceeding the expected normal range for a 15-year-old adolescent (approximately 220–250g). This enlargement was characterized by left ventricular hypertrophy and diffuse fibrous thickening of both the mitral and aortic valves. The myocardium was pale and soft upon sectioning, consistent with chronic degenerative changes (Figure 2a).

In the ascending aorta, the intimal surface exhibited multiple longitudinal yellow streaks "fatty streaks", indicating early lipid deposition within the subendothelial layer (Figure 2b).

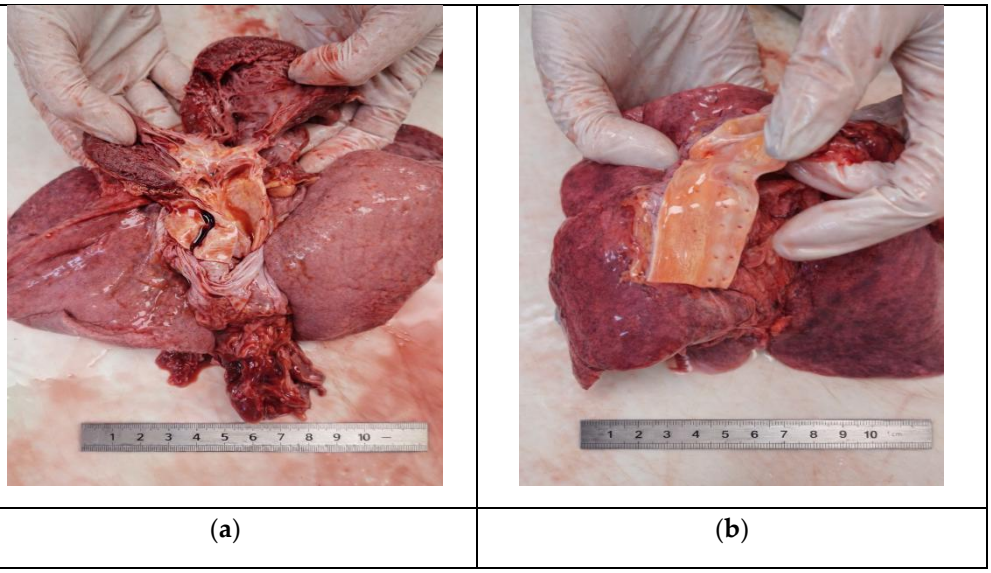

(**a**) (**b**)

Figure 2. Macroscopic cardiac and vascular findings: **(a)** cardiomegaly, left ventricular hypertrophy, fibrous thickening of the mitral and aortic valves**, (b)** early-lipid streaks (ascending aorta).

The lungs were increased in weight (total approximately 950g; reference range for age: 750–900g), and appeared heavy, congested, and edematous, releasing serohemorrhagic foamy fluid on cut surface, with multifocal inflammatory consolidation consistent with bronchopneumonia (Figure 3 and 3b).

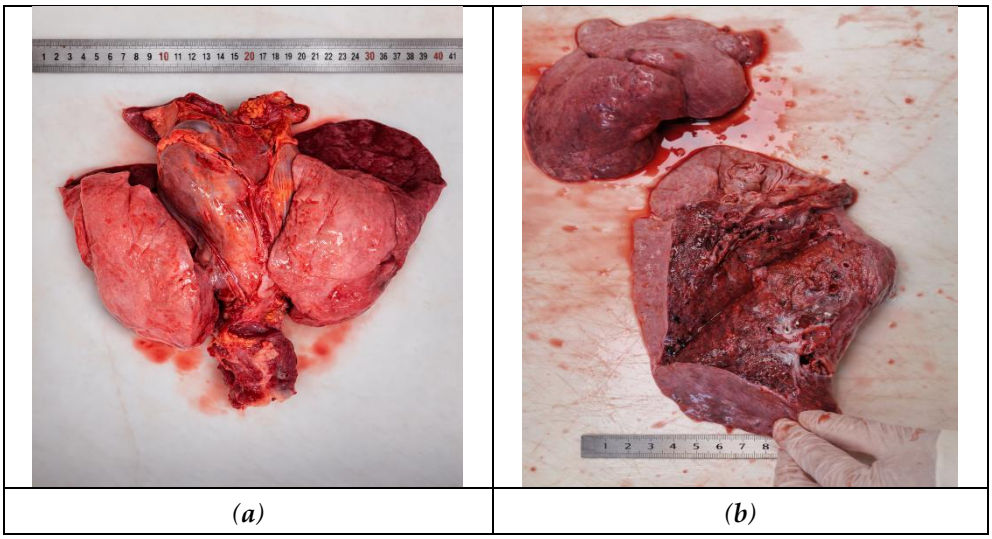

(*a*) (*b*)

Figure 3. Gross appearance of the lungs: (a) congestion and dark-red pleural discoloration, (b) serohemorrhagic foamy fluid, with multifocal inflammatory consolidation.

The liver was moderately enlarged and weighed approximately 1600 g (normal range for age: 1200–1400 g), with firm consistency and homogeneous appearance (Figure 4a), while the spleen

 doi:10.20944/preprints202603.2091.v1

demonstrated moderate splenomegaly, with a weight of approximately 220g (normal range for age: 120–150g), indicating systemic lysosomal storage disease (Figure 4b).

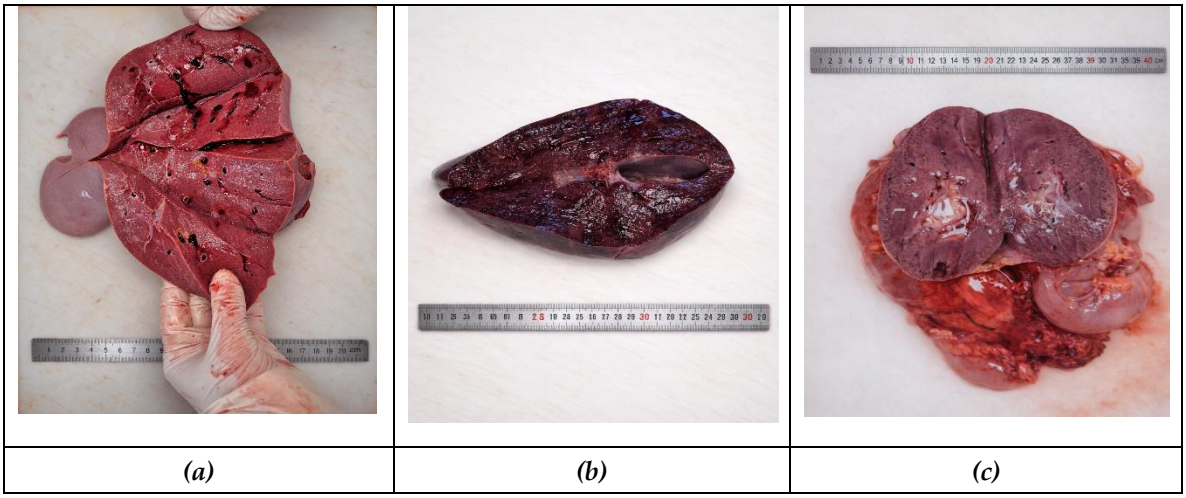

(a) *(b)* *(c)*

Figure 4. Macroscopic examination of abdominal organs: **(a)** liver showing diffuse dark-red congestion and parenchymal alterations, **(b)** spleen displaying enlargement and congestive appearance, **(c)** kidney with dark cortical discoloration and congestive parenchyma.

The kidneys demonstrated diffuse parenchymal congestion and mild interstitial edema, although corticomedullary differentiation remained preserved, weighing approximately 160 g (right) and 170 g (left) (reference range for age: 110–130 g) (Figure 4c).

The gastrointestinal tract exhibited erosive inflammatory lesions involving the gastroesophageal and intestinal mucosa. The gastrostomy site showed no macroscopic complications and no signs of local inflammation. Overall, the macroscopic findings were consistent with advanced multisystem metabolic disease with terminal cardiorespiratory decompensation. The mesenteric lymph nodes were enlarged due to the accumulation of macrophages containing stored GAGs.

3.2. Microscopic Findings

Histological examination revealed diffuse cytoplasmic vacuolization affecting multiple tissues, characterised by lysosomal storage disorders.

Within the central nervous system, neurons and glial cells showed prominent cytoplasmic vacuolization, interstitial edema, and early leukoencephalopathic changes, the latter representing a morphological indicator of advanced neurodegeneration (Figure 5a and 5b).

In the cerebellum, cortical and subcortical neurons show marked cytoplasmic ballooning and fine-to-coalescent vacuolization, consistent with intralysosomal accumulation of glycosaminoglycans (predominantly heparan sulfate). These changes are accompanied by neuropil rarefaction with a mild spongiform appearance, focal neuronal loss, microglial activation, and reactive gliosis.

Enlarged Purkinje cells have pale, vacuolated cytoplasm and degenerative changes, associated with decreased neuronal density, granular layer disorganization, and gliosis, reflecting progressive lysosomal storage–related neurodegeneration (Figure 5c).

 doi:10.20944/preprints202603.2091.v1

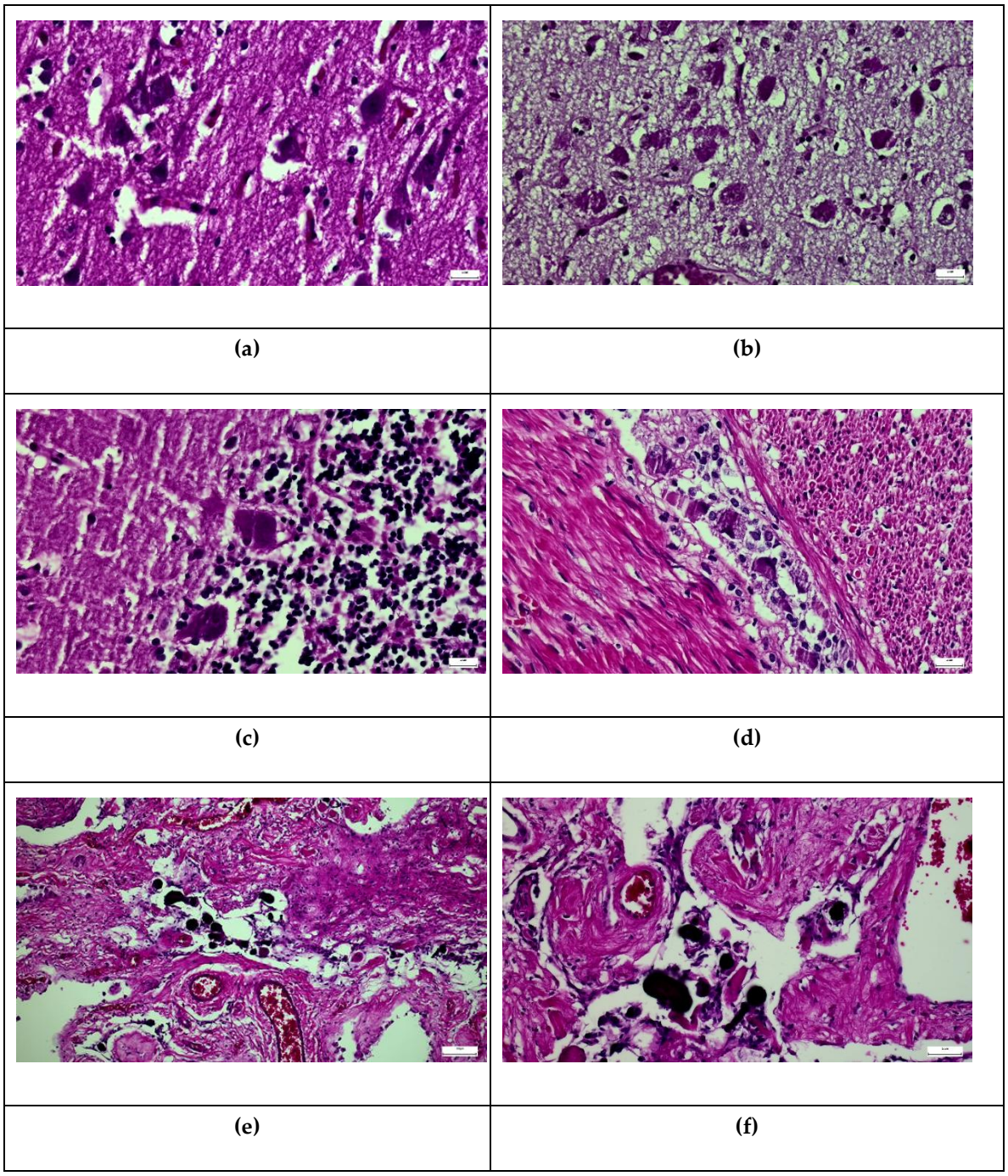

Figure 5. Histopathology of the organs after autopsy utilizing hematoxylin and eosin (HE) and PAS staining: (i) brain show cytoplasmic vacuolization of the neurons and glial cells (HE×40):**(a)** and (PASx40):**(b)**; (ii) cerebellum shows enlarged Purkinje cells with pale vacuolated cytoplasm and degenerative changes (HE×40): **(c)**; (iii) myenteric ganglion shows neuronal enlargement with cytoplasmic vacuolization,: (HE×40) **(d)**; choroid plexus reveals stromal alterations with scattered microcalcifications distributed in perivascular areas (HEx20): **(e)** and (HEx40): **(f)**.

In the colon in the myenteric (Auerbach) plexus, enteric ganglion neurons display prominent somatic distension and extensive cytoplasmic vacuolization ("ballooning degeneration"), occasionally with reduced neuronal density and perineural glial reaction, indicating involvement of the peripheral autonomic nervous system (Figure 5d).

Microcalcifications were also present in the brain, cerebellum, and predominantly perivascular choroid plexuses (Figure 5e-5f).

 doi:10.20944/preprints202603.2091.v1

Overall, the combined features demonstrate multisystem cardiac involvement in MPS III, characterized by intracellular storage in cardiomyocytes together with progressive interstitial fibrosis, contributing to myocardial stiffening, impaired contractility, and long-term cardiomyopathic changes.

Myocardial fibres show cytoplasmic vacuolization and sarcoplasmic clearing consistent with lysosomal glycosaminoglycan accumulation within cardiomyocytes. Myocyte hypertrophy with architectural disarray, interstitial edema, and focal myofibrillar rarefaction are observed, reflecting progressive storage-related cellular dysfunction and early myocardial remodeling (Figure 6a and 6b).

Masson's trichrome staining: increased subendocardial and interstitial and perivascular collagen deposition (green staining) highlights diffuse and patchy myocardial fibrosis, separating and entrapping cardiomyocytes (red) (Figure 6c and 6d).

These findings indicate chronic extracellular matrix remodeling and replacement fibrosis secondary to prolonged metabolic injury.

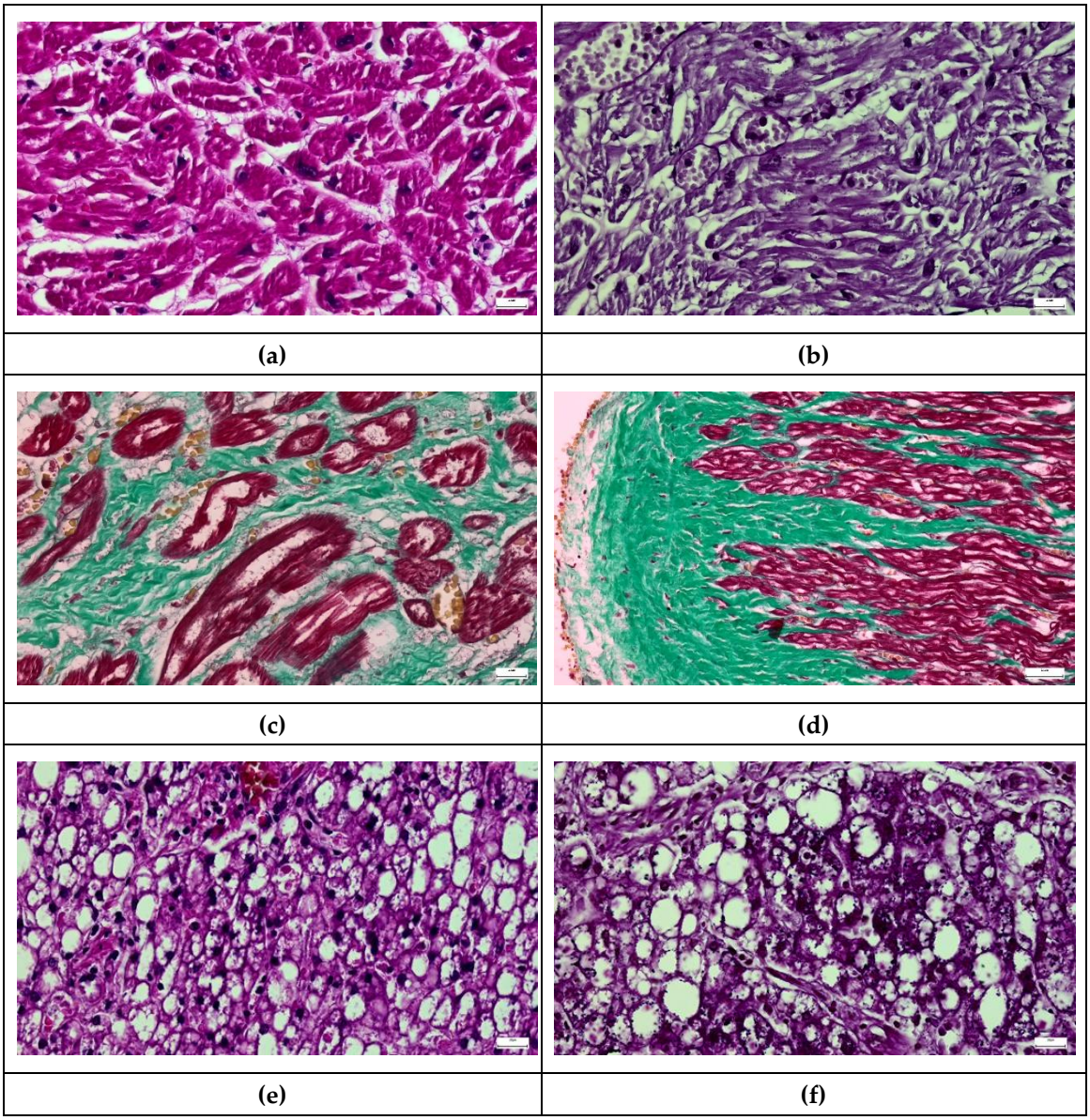

Figure 6. Histopathology of the organs after autopsy utilizing hematoxylin and eosin (HE), PAS and Masson's trichrome stains unveil: (i) cardiac histopathological alterations show cardiomyocyte vacuolization in cross section (HEx40): **(a)** and in longitudinal section (PASx40): **(b)**); (ii) cardiac histopathological alterations reveal interstitial and subendocardial myocardial fibrosis (Masson's trichrome x40:**(c)** and Masson's trichrome

 doi:10.20944/preprints202603.2091.v1

x20):**(d)**); (iii) liver histopathological alterations reveal hepatocytes with marked cytoplasmic vacuolization and cytoplasmic inclusions (HEx20: **(e)** and PASx40: **(f)**).

In the liver, hepatocytes and Kupffer cells were enlarged with clear vacuolated cytoplasm, corresponding to intralysosomal glycosaminoglycan accumulation (Figure 6e and 6f).

Histological analyses revealed diffuse parenchymal damage with extensive cytoplasmic clearing of hepatocytes, resulting in a foamy, microvacuolized appearance and slight architectural disorganization of the hepatic cords. Portal and sinusoidal regions showed swollen hepatocytes with prominent intracellular vacuoles consistent with lysosomal glycosaminoglycan accumulation, associated with sinusoidal narrowing and mild stromal reaction.

Ballooned hepatocytes were identified with coarse cytoplasmic vacuolization and displacement of nuclei, reflecting progressive lysosomal distension and metabolic storage injury, also extensive intracytoplasmic storage vacuoles within hepatocytes and Kupffer cells, producing marked cellular enlargement and parenchymal rarefaction.

Overall, these findings demonstrate diffuse visceral (hepatic) involvement in MPS III, characterized by intralysosomal glycosaminoglycan accumulation in hepatocytes and Kupffer cells, leading to hepatocellular swelling, sinusoidal compression, and progressive organ dysfunction.

Similar vacuolar changes were observed in renal tubular epithelial cells, pancreatic acinar cells showed similar microvacuolation without signs of chronic pancreatitis, and enteric ganglion cells.

Microscopic analyses showed diffuse involvement of the renal parenchyma with cytoplasmic clearing and microvacuolar change affecting tubular epithelial cells, resulting in a pale, foamy appearance and mild architectural distortion (Figure 7a and 7b). Were also present swollen tubular epithelial cells with prominent intracytoplasmic vacuoles consistent with lysosomal glycosaminoglycan accumulation, associated with tubular luminal narrowing and interstitial congestion (Figure 7a), marked ballooning degeneration of epithelial cells with optically clear storage vacuoles and nuclear displacement, reflecting lysosomal distension and progressive metabolic storage injury (Figure 7b).

These findings support renal involvement in MPS III, characterized by intracellular lysosomal storage within tubular epithelium and interstitial cells, contributing to tubular dysfunction and progressive parenchymal alteration.

The spleen and lymph nodes showed sinusoidal congestion and prominent histiocytosis with foamy macrophages. (Figure 7c-7f).

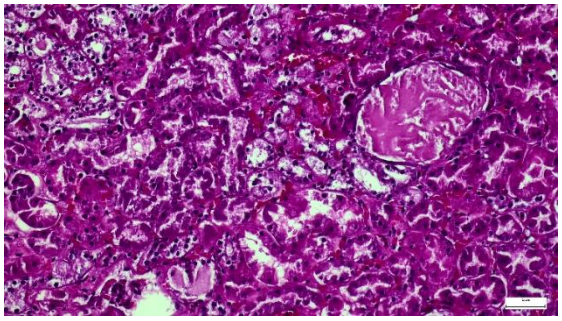

(a)

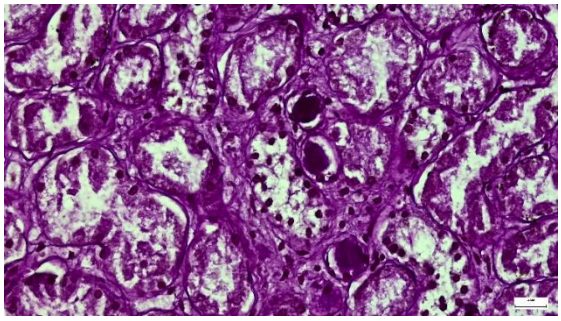

(b)

 doi:10.20944/preprints202603.2091.v1

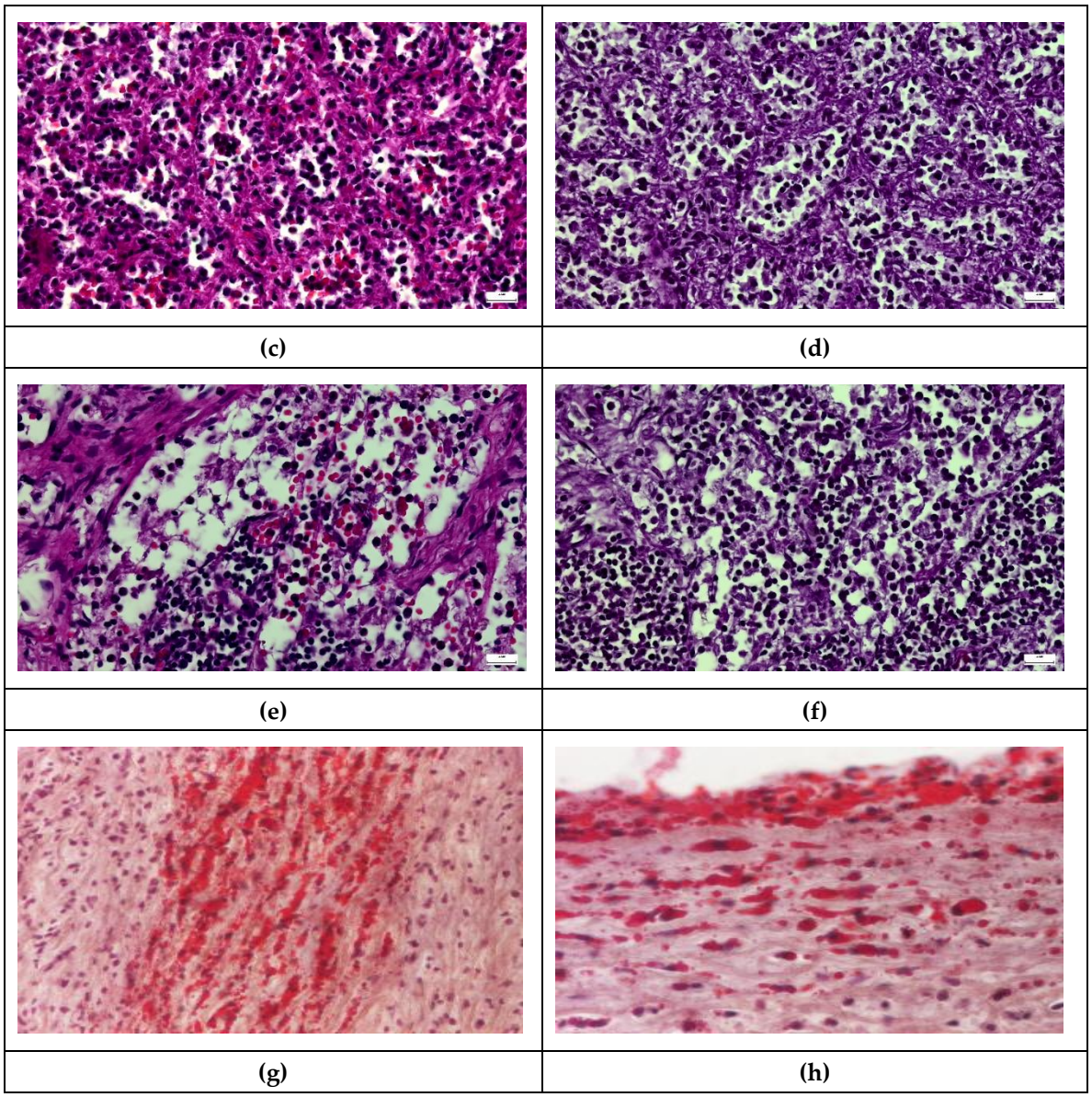

Figure 7. Histopathology of the organs after autopsy utilizing hematoxylin and eosin (HE), PAS and Scharlach stains unveil: (i) renal parenchymal histopathological changes reveal tubular epithelial vacuolization and cytoplasmic inclusions mixed with interstitial calcifications (HEx20: **(a)** and PASx40: **(b)**); (ii) spleen parenchymal histopathological changes show vacuolated macrophages within the splenic parenchyma and cytoplasmic inclusions (HE x20: **(c)** and PASx20: **(d)**); (iii) lymph node parenchymal histopathological changes reveal histiocytic cells with cytoplasmic vacuolization and cytoplasmic inclusions (HEx40: **(e)** and PASx40: **(f)**); (iv) the aortic intima show lipid-laden macrophages in the intimal layer and foamy macrophages with intracellular lipid deposits (Scharlach x20: **(g)** and x40: **(h)**).

At the vascular level, the aortic intima revealed subendothelial aggregates of foamy macrophages arranged in bands and nests, positive for lipid staining (Scharlach stain), consistent with early atherogenic “fatty streak” lesions.

Microscopic examination reveals aggregates of foamy macrophages arranged in bands and nests within the subendothelial tissue. These cells show positive Scharlach staining, confirming intracellular lipid accumulation (Figure 7g and 7h). Representative microscopic fields at progressively higher magnifications illustrating the distribution and density of lipid-laden macrophages in the aortic intima.

These findings confirm widespread lysosomal storage pathology with prominent multisystem involvement, accompanied by secondary vascular lipid accumulation.

 doi:10.20944/preprints202603.2091.v1

4. Discussion

Mucopolysaccharidosis type III (MPS III) is clinically defined by its devastating neurodegenerative course, a feature that often overshadows its systemic impact. However, while the central nervous system remains the primary focus of clinical management, the underlying pathophysiology involves a silent, progressive accumulation of glycosaminoglycans across multiple organ systems [3,4].

As emerging therapies like enzyme replacement and gene editing begin to reshape the treatment landscape for lysosomal storage disorders, accurately mapping the systemic distribution of pathology becomes crucial.

We report the case of a 15-year-old patient, an age that represents an advanced stage of MPS III. This longevity provides a unique opportunity to document the extensive visceral pathology that often progresses silently beneath the dominant neurodegenerative phenotype.

The widespread cytoplasmic vacuolization observed across visceral organs reflects progressive intralysosomal glycosaminoglycan accumulation, a hallmark of lysosomal storage disorders [2,7,21,22], lesions that have also been reported in other studies [6,13]. Lysosomal distension disrupts intracellular metabolism, promotes chronic inflammation, and activates apoptotic pathways, ultimately leading to progressive tissue dysfunction [2,7]. Similar multisystem histopathological lesions have been reported in previous morphopathological studies of MPS patients [6,13].

While neurological deterioration defines the clinical course [8,10], visceral involvement plays a significant role in morbidity and mortality [9,14,23], with similar lesions also identified in our patient. In advanced stages, aspiration bronchopneumonia and cardiorespiratory failure represent frequent terminal events [17].

In our case, gross examination revealed enlarged and heavy lungs with diffuse congestion and marked pulmonary edema; on sectioning serohemorrhagic foamy fluid was released, and focal areas of consolidation consistent with aspiration bronchopneumonia were observed. The heart showed cardiomegaly, chamber dilatation, and atrioventricular valvular thickening, while the myocardium appeared pale and soft, suggestive of myocardial degeneration associated with interstitial fibrosis. In mucopolysaccharidosis type III, cardiac involvement is commonly associated with glycosaminoglycan deposition in the valves and conduction system, contributing to cardiac dysfunction. The liver was moderately enlarged and exhibited chronic passive congestion, indicating systemic venous stasis. These macroscopic findings support the occurrence of acute cardiorespiratory decompensation in the context of gradual multisystem involvement. Additionally, structural cardiac abnormalities, including myocardial degeneration and valvular thickening, further contributed to hemodynamic instability [12,18,19,21].

Compared with MPS types I and II, where somatic manifestations are clinically conspicuous and frequently guide early diagnosis and follow-up [1,15,16], systemic involvement in MPS III is often underestimated during life [4]. In these patients, the predominance of severe and rapidly progressive neurocognitive decline tends to overshadow extracerebral disease [8,9], diverting clinical attention away from visceral pathology. As a consequence, glycosaminoglycan accumulation within the liver, spleen, heart, kidneys, and reticuloendothelial tissues may progress silently, producing subtle or nonspecific manifestations that remain clinically underrecognized [13,14].

Comprehensive post-mortem analysis evaluation, therefore, represents critical tool for accurately mapping the true extent of multisystem involvement, providing direct morphologic evidence of storage burden and organ-specific vulnerability [2,22]. Such post-mortem findings not only enhance our understanding of disease pathogenesis and natural history but also have important translational implications. In particular, defining the tissue distribution and severity of storage pathology may inform emerging therapeutic strategies, including enzyme replacement therapy and gene therapy [23–25], by identifying target organs, therapeutic windows, and potential barriers to effective systemic delivery.

In addition, early lipid-rich intimal streaks with subendothelial foamy macrophages were observed in the aorta. Although MPS III is primarily characterized by glycosaminoglycan storage

 doi:10.20944/preprints202603.2091.v1

rather than primary lipid deposition, global lysosomal dysfunction may secondarily disturb cellular lipid turnover and promote foam cell formation.

Prolonged immobilization in advanced stages of the disease may promote chronic venous stasis, which likely contributed to the chronic passive hepatic congestion observed at post-mortem analysis.

Chronic systemic inflammation, metabolic imbalance, and prolonged immobilization associated with severe lysosomal storage disease may further contribute to early atherogenic vascular changes. Also, prolonged immobilization in advanced stages of the disease may promote chronic venous stasis, which likely contributed to the chronic passive hepatic congestion observed at post-mortem analysis.

Similar mechanisms of secondary lipid accumulation and inflammatory activation have been described in lysosomal storage disorders, linking lysosomal dysfunction to altered lipid homeostasis and vascular pathology [26–28]. In the context of terminal-stage disease and palliative care, recognition of systemic involvement - especially gastrointestinal and cardiac manifestation - is essential for optimizing symptom control and improving quality of life in patients with advanced MPS III.

The observed aortic lipid deposition underscores a cross-talk between glycosaminoglycan accumulation and disrupted lipid homeostasis, likely exacerbated by chronic systemic inflammation and prolonged immobility

5. Conclusions

Mucopolysaccharidosis type III is best understood as a systemic and progressive lysosomal storage disorder with widespread multisystem involvement, rather than an exclusively neurodegenerative disease. Recognition of these systemic alterations supports the need for a multidisciplinary approach, extending beyond purely neurological management, even in advanced stages of the disease. The present case of a 15-year-old patient of relatively advanced age for the severe clinical spectrum of MPS III provided a unique opportunity to document the full morphological extent of the disease. Survival into adolescence, likely facilitated by comprehensive palliative care, allowed for the observation of extensive intralysosomal glycosaminoglycan accumulation across the central nervous system, cardiovascular structures, and visceral organs.

The presence of early lipid-rich aortic intimal streaks suggests secondary vascular lipid accumulation related to global lysosomal dysfunction and chronic inflammation. While not disease-specific, these changes, captured at an advanced stage of disease progression, expand the known morphological spectrum of MPS III

Comprehensive clinicopathological correlation through post-mortem analysis remains essential for accurately delineating disease extent and clarifying mechanisms of terminal decompensation. Such findings are crucial for informing future systemic therapeutic strategies that must target both neurological and extracerebral pathology to address the total disease burden.

Author Contributions: Conceptualization, M.F.T. and L.L.; methodology, M.F.T., L.L. and V.T.; software, C.I.S., I.F. and L.G.B.; validation, M.F.T., L.L. and E.R.A.; formal analysis, I.F. and N.F.; investigation, M.F.T., L.L. and E.R.A; resources, V.T., N.F. and D.T.A.-P.; data curation, S.M.M. and D.T.A.-P.; writing—original draft preparation, M.F.T., L.L. and V.T.; writing—review and editing, L.L., E.R.A, and S.M.M.; visualization, M.T.F. and E.R.A.; supervision, L.L.; project administration, L.L. and L.G.B.; All authors have read and agreed to the published version of the manuscript.

Funding: This research received no external funding.

Institutional Review Board Statement: The study was conducted in accordance with the Declaration of Helsinki and approved by the Ethics Committee of Children's Emergency Hospital "Sf. Maria" in Iași (No. 9899; 4 March 2026), for studies involving humans.

Informed Consent Statement: Written informed consent was obtained from the patient's legal guardians for the publication of this case report and any accompanying images.

 doi:10.20944/preprints202603.2091.v1

Data Availability Statement: The original contributions presented in this study are included in the article/supplementary material. Further inquiries can be directed to the corresponding author.

Conflicts of Interest: The authors declare no conflicts of interest.

References

1. Benetó, N.; Vilageliu, L.; Grinberg, D.; Canals, I. Sanfilippo syndrome: Molecular basis, disease models and therapeutic approaches. *Int. J. Mol. Sci.* **2020**, 21, 7819. https://doi.org/10.3390/ijms21217819
2. Viana, G.M.; Priestman, D.A.; Platt, F.M.; Khan, S.; Tomatsu, S.; Pshezhetsky, A.V. Brain pathology in mucopolysaccharidoses. *J. Clin. Med.* **2020**, 9, 395. https://doi.org/10.3390/jcm9020395
3. Delgadillo, V.; O'Callaghan, M.d.M.; Gort, L.; Coll, M.J.; Pineda, M. Natural history of Sanfilippo syndrome in Spain. *Orphanet J. Rare Dis.* **2013**, 8, 189. https://doi.org/10.1186/1750-1172-8-189
4. Wijburg, F.A.; Węgrzyn, G.; Burton, B.K.; Tylki-Szymańska, A. Mucopolysaccharidosis type III (Sanfilippo syndrome) and misdiagnosis of idiopathic developmental delay, attention deficit/hyperactivity disorder or autism spectrum disorder. *Acta Paediatr.* **2013**, 102, 462–470. https://doi.org/10.1111/apa.12169
5. Wiśniewska, K.; Wolski, J.; Zabi ´nska, M.; Szulc, A.; Gaffke, L.; Pierzynowska, K.; W˛egrzyn, G. Mucopolysaccharidosis Type IIIE: A Real Human Disease or a Diagnostic Pitfall? *Diagnostics* **2024**, 14, 1734. https://doi.org/10.3390/diagnostics14161734
6. Valstar, M.J.; Marchal, J.P.; Grootenhuis, M.A.; Colland, V.T.; Wijburg, F.A. Cognitive development in patients with mucopolysaccharidosis type III (Sanfilippo syndrome). *Orphanet J. Rare Dis.* **2011**, 6, 43. https://doi.org/10.1186/1750-1172-6-43
7. Rouse, C.J.; Jensen, V.N.; Heldermon, C.D. Mucopolysaccharidosis type IIIB: A current review and exploration of the AAV therapy landscape. *Neural Regen. Res.* **2023**, 19, 355–359. https://doi.org/10.4103/1673-5374.377606
8. Lorenz, D.; Musacchio, T.; Kunstmann, E.; Grauer, E.; Pluta, N.; Stock, A.; Speer, C.P.; Hebestreit, H. A case report of Sanfilippo syndrome—the long way to diagnosis. *BMC Neurol.* **2022**, 22, 93. https://doi.org/10.1186/s12883-022-02611-7
9. Poswar, F.O.; Santos, H.S.; Santos, A.B.S.; Berger, S.V.; de Souza, C.F.M.; Giugliani, R.; Baldo, G. Progression of cardiovascular manifestations in adults and children with mucopolysaccharidoses with and without enzyme replacement therapy. *Front. Cardiovasc. Med.* **2022**, 8, 801147. https://doi.org/10.3389/fcvm.2021.801147
10. Rosser, B.A.; Chan, C.; Hoschtitzky, A. Surgical management of valvular heart disease in mucopolysaccharidoses: A review of literature. *Biomedicines* **2022**, 10, 375. https://doi.org/10.3390/biomedicines10020375
11. Hampe, C.S.; Eisengart, J.B.; Lund, T.C.; Orchard, P.J.; Swietlicka, M.; Wesley, J.; McIvor, R.S. Mucopolysaccharidosis type I: A review of the natural history and molecular pathology. *Cells* **2020**, 9, 83. https://doi.org/10.3390/cells9020083
12. Nan, H.; Chanbum, P.; Maeng, S. Mucopolysaccharidoses I and II: Brief review of therapeutic options and supportive/palliative therapies. *Biomed Res. Int.* **2020**, 2020, 2408402. https://doi.org/10.1155/2020/2408402
13. Scarpa, M.; Orchard, P.J.; Schulz, A.; Dickson, P.I.; Haskins, M.E.; Escolar, M.L.; Giugliani, R. Treatment of brain disease in the mucopolysaccharidoses. *Mol. Genet. Metab.* **2017**, 122, 25–34. https://doi.org/10.1016/j.ymgme.2017.10.007
14. Montanari, C.; Tagi, V.M.; D'Auria, E.; Guaia, V.; Di Gallo, A.; Ghezzi, M.; Verduci, E.; Fiori, L.; Zuccotti, G. Lung diseases and rare disorders: Is it a lysosomal storage disease? Differential diagnosis, pathogenetic mechanisms and management. *Children (Basel)* **2024**, 11, 668. https://doi.org/10.3390/children11060668
15. Lipiński, P.; Różdżyńska-Świątkowska, A.; Wiśniewska, K.; Rusecka, J.; Ługowska, A.; Żuber, Z.; Jezela-Stanek, A.; Cyske, Z.; Gaffke, L.; Pierzynowska, K.; Węgrzyn, G.; Tylki-Szymańska, A. Mucopolysaccharidoses—What clinicians need to know: A clinical, biochemical, and molecular overview. *Biomolecules* **2025**, 15, 1448. https://doi.org/10.3390/biom15101448
16. Gürbüz, B.B.; Aypar, E.; Alehan, D.; Öner, Ö.; Teber, S.; Ünal, Ö.; Tuncel, T. Evaluation of cardiac findings in mucopolysaccharidosis type III patients. *J. Pediatr. Res.* **2021**, 8, 195–201.

 doi:10.20944/preprints202603.2091.v1

17. Valstar, M.J.; Ruijter, G.J.G.; van Diggelen, O.P.; Poorthuis, B.J.; Wijburg, F.A. Sanfilippo syndrome: A mini-review. *J. Inherit. Metab. Dis.* **2008**, 31, 240–252. https://doi.org/10.1007/s10545-008-0838-5
18. Clark, B.M.; Sprung, J.; Weingarten, T.N.; Warner, M.E. Anesthesia for patients with mucopolysaccharidoses: Comprehensive review with emphasis on airway management. *Bosn. J. Basic Med. Sci.* **2018**, 18, 1–7. https://doi.org/10.17305/bjbms.2017.2201
19. Romagnoli, A.S.; Campos, L.N.; Fernandez-Guzman, D.; Wagemaker, S.; Fernandez Zelcer, F.; Stegmann, C.; Argüelles, C.F.; Sosa, L.F.; Gerk, A.; Stegmann, J. Evaluating patients with mucopolysaccharidosis type III: A scoping review on diagnostic and follow-up approaches. *J. Appl. Res. Intellect. Disabil.* **2025**, 38, e70024. https://doi.org/10.1111/jar.70024
20. Neufeld, E.F.; Muenzer, J. The mucopolysaccharidoses. In: Scriver, C.R.; Beaudet, A.L.; Sly, W.S.; Valle, D., Eds.; The Metabolic and Molecular Bases of Inherited Disease; McGraw-Hill: New York, NY, USA, 2001.
21. Parenti, G.; Andria, G.; Ballabio, A. Lysosomal storage diseases: From pathophysiology to therapy. *Annu. Rev. Med.* **2015**, 66, 471–486. https://doi.org/10.1146/annurev-med-122313-085916
22. Platt, F.M.; d'Azzo, A.; Davidson, B.L.; Neufeld, E.F.; Tifft, C.J. Lysosomal storage diseases. *Nat. Rev. Dis. Primers.* **2018**, 4, 27. https://doi.org/10.1038/s41572-018-0025-4
23. Braunlin, E.A.; Harmatz, P.R.; Scarpa, M.; Furlanetto, B.; Kampmann, C.; Loehr, J.P.; Ponder, K.P.; Roberts, W.C.; Rosenfeld, H.M.; Giugliani, R. Cardiac disease in patients with mucopolysaccharidoses: Presentation, diagnosis and management. *J. Inherit. Metab. Dis.* **2011**, 34, 1183–1197. https://doi.org/10.1007/s10545-011-9359-8
24. Beck, M. Treatment strategies for lysosomal storage disorders. *Dev Med Child Neurol.* **2018**, 60, 13–18. https://doi.org/10.1111/dmcn.13600
25. Parenti, G.; Medina, D.L.; Ballabio, A. The rapidly evolving view of lysosomal storage diseases. *EMBO Mol Med*. **2021**, 13, e12836. https://doi.org/10.15252/emmm.202012836
26. Platt, F.M.; Boland, B.; van der Spoel, A.C. The cell biology of disease: lysosomal storage disorders: the cellular impact of lysosomal dysfunction. *J Cell Biol.* **2012**; 199(5):723–734. doi:10.1083/jcb.201208152
27. Libby, P. Inflammation in atherosclerosis. *Nature.* **2002**; 420(6917), 868–874. doi:10.1038/nature01323
28. Napoli, C.; Glass, C.K.; Witztum, J.L.; Deutsch, R.; D'Armiento, F.P.; Palinski, W. Influence of maternal hypercholesterolemia during pregnancy on progression of early atherosclerotic lesions in childhood: fate of early lesions in children (FELIC) study. *Lancet.* **1999**; 354(9186), 1234–1241. doi:10.1016/S0140-6736(99)02131-5.